

# INFLUENCE OF LASER POWER ON MICROHARDNESS AND WEAR RESISTANCE PROPERTIES OF LASER METAL DEPOSITED 17-4 PH STAINLESS STEEL

A. Adeyemi<sup>1</sup>, E. T. Akinlabi<sup>1</sup>, and R. M. Mahamood<sup>1, 2,\*</sup>

<sup>1</sup>Department of Mechanical Engineering Science, University of Johannesburg, Auckland Park, Kingsway Campus, Johannesburg, 2006, South Africa

<sup>2</sup>Department of Mechanical Engineering University of Ilorin, Ilorin, 23400003, Nigeria

\* Corresponding author's e-mail address: mahamoodmr2009@gmail.com

## ABSTRACT

*This aim of this research is to investigate the impact of laser power on the hardness and the wear resistance properties of laser metal deposited 17-4 PH stainless steel. Hardness was studied using Zwick/Roell microhardness tester and the wear resistance property was carried out using ball-on-disc Anton Paar-tribometer wear tester. The study revealed that an irregular increase and decrease in the average hardness value and wear behaviour were observed. This could be attributed to the presence of copper precipitate which was more concentrate at the overlapping region because of the reheating activity that is happening between the succeeding and preceding track layers.*

**KEYWORDS:** Laser Metal Deposition, Laser Power, 17-4 PH stainless steel, Microhardness, Wear resistance.

## 1. INTRODUCTION

The precipitation-hardened martensitic stainless steel was developed as a compromise between the fully austenitic and fully martensitic stainless steels for optimum properties such as: strength, ductility, and toughness [1]. Precipitation-hardened stainless steel has been favoured in industries as a choice structural material. Industrial applications of Precipitation-hardened stainless steel include: turbine blade in aerospace industry, for marine parts, and petrochemical industries due to its excellent properties [1, 2]. The strengthening property of Precipitation-hardened stainless steel is as a result of copper precipitates produced during ageing process [1]. The 17 stands for the approximate weight percentage composition of chromium (Cr) that makes the steel to have high corrosion resistance property while the 4 stands for the approximate weight percentage composition of Nickel (Ni). Other composition elements include silicon, niobium and molybdenum. These compositions and the heat treatment that the steel was subjected to give it the characteristic property that makes the steel an important material used various applications. Despite these exciting properties, Precipitation-hardened stainless steel belongs to the class of difficult to machine materials as a result of high cutting temperatures generated that accumulates the

cutting zone. This high temperature causes the cutting tool to be damaged which in turn degrades the surface finish produced. Hence an alternative manufacturing process is desired for this and other difficult to machine materials.

Additive manufacturing (AM) method is an excellent alternative manufacturing technology for difficult to machine materials because it is a tool-less manufacturing process [3 -5]. Additive manufacturing process achieve manufacturing of components by building the material up from the three dimensional (3D) computer aided design (CAD) model of the component in layers. There different types of AM technologies that include: selective laser sintering/melting, fused deposition modelling and laser metal deposition process [6 – 10].

Laser metal deposition (LMD) process is an additive manufacturing technique where solid components are manufactured by deposition of powder or wire in a layer-wise configuration onto a melt pool created on a substrate by high intensity laser beam. After solidification, a solid track as well as layers of material is seen which forms a fully functional component based on the 3D CAD data [11, 12]. The LMD process is useful in fabrication of complex, repair and remanufacturing of existing parts and ability to manufacture part consisting of composite and functionally graded materials [13-15]. LMD process is governed by several processing parameters that

---

include: laser power, scanning speed, gas flow rate, powder feed rate, and laser spot size. The processing parameters have been reported in the literature to have a significant influence on the quality of the built part using the LMD process which includes: metallurgical, mechanical and physical properties [16].

Several investigations have been reported in the literature on how processing parameters affects the properties of laser metal deposited stainless steel [17-27]. Yu and Maes [17] investigated how processing parameters affects the cracking behaviour and mechanical properties of a laser metal deposited austenitic stainless steel grade. The processing parameters considered in this study are: the laser power, scan speed, spot diameter, powder feed rate and overlap percentage. The result showed that, the porosity can be eliminated by increasing the laser power and this will also prevent crack formation in the deposited austenitic stainless steel. A similar study was conducted by Zhang et al. [18]. The authors studied how processing parameters affects microstructure, hardness and tensile strength of laser metal deposited 316 stainless steel. The processing parameters studied are the scanning speed and the laser power. The result of this investigation revealed that the scanning speed has a great influence on the temperature intensity, solidification rate and the geometrical characteristics of the deposited stainless steel. Yadollahi et al [19] investigated how processing parameters of laser power, powder feed rate, and scanning speed affect the mechanical properties of laser metal deposited stainless steel. A very strong correlation between the laser power and structural properties of the 316L stainless steel was observed in this study. Guo et al. [20] studied the influence of laser power on the microstructure and the mechanical property of stainless steel 316L. The result revealed was similar to that of observed by Zhang et al. [18] discussed earlier. High laser power was found to cause an increase in the geometrical properties and reduction on solidification rate thereby producing defect free microstructure and improved mechanical properties.

Wang et al [21] also investigated the influence of the laser power on anisotropic, heterogeneous and tensile properties of laser metal deposited 304L stainless steel. The study revealed that the laser power has a great influence on the tensile and ductility property of laser metal deposited 304L stainless steel. Bayode et al [22] investigated how laser power affects the microstructure and microhardness property of 316L stainless steel that was produced using the laser metal deposition process. The result showed that the hardness property increases with decrease in laser power due to the formation of fine microstructural of delta ( $\delta$ ) ferrite stringers, while the hardness property was found to decrease as the laser power was increased due to the formation of coarse microstructural delta ferrite stringers. Bayode et al. [23] also reported the influence of scanning speed on the property of laser metal deposited 17-4 PH stainless steel. The authors found

that the that structural integrity of the laser metal deposited 17-4 PH stainless steel increases with increase in scanning speed. In this study, the influence of laser power on the microhardness and wear resistance property of laser metal deposited 17-4 PH stainless steel was investigated. The laser power was varied from 1000 W and 2600 W.

## 2. MATERIALS AND METHODS

The experimental study of the laser metal deposition process was carried out using Nd-YAG laser attached to a Kuka robot with maximum laser capacity of 4000 W and wavelength of 1.06 microns. The 17-4 PH stainless steel powder was used in this study and it is 99.8% pure. The 17-4 PH stainless steel powder is of particle size range of between 45 and 90  $\mu\text{m}$ . The 17-4PH powder was deposited on a 316 stainless steel substrate with dimensions of 100 x 100 x 10 mm. Before the deposition process, the substrate was prepared through sandblasting and then cleaned with acetone to achieve better laser absorption. The powder was delivered onto the substrate through coaxial powder delivery system. During the deposition process, multiple tracks of 17-4 PH stainless steel powder were produced at 50% overlap percentage. The powder was fed unto the melt pool that was created on the 316 stainless steel substrate by the laser beam. The Laser power was varied between 1000 W to 2600 W. Other processing parameters: the scanning speed, powder flow rate and gas flow rate which were fixed throughout the experiment at 1.2 m/min, 5 g/min and 2 l/min respectively. The experimental set-up of the laser metal deposition process is shown in Figure 1a and the schematic diagram of LMD process is shown in Figure 1b. The elemental composition of 17-4 PH stainless steel used in this experiment is presented in Table 1.



(a)

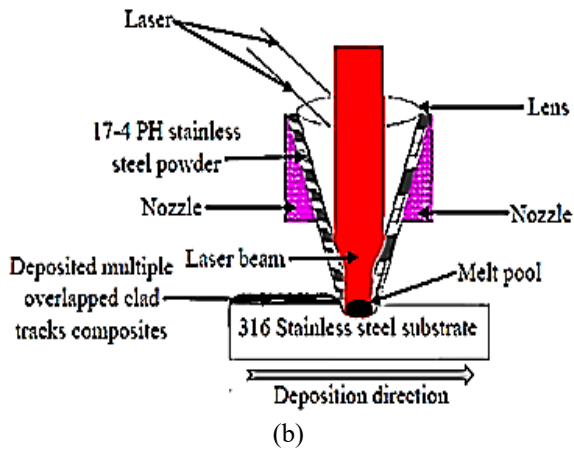


Fig. 1. The (a) Experimental set-up (b) Schematic Diagram of the LMD process

Table 1. Elemental Composition of 17-4 PH Stainless Steel Powder

Element	Composition (%)
Silicon (Si)	0.78
Chromium	17.81
Manganese (Mn)	1.27
Iron (Fe)	72.26
Nickel (Ni)	4.20
Copper (Cu)	3.19
Others	Balance

### 2.1. Microstructural Examination

The deposited samples were cut laterally and prepared for characterization according to ASTM E3- 11. The cut specimens were mounted in polyfast through hot mounting press. The mounted samples were grounded, polished and etched using Kalling's reagent which comprises of 100 ml hydrochloric acid, 100 ml ethanol and 5 g cupric chloride. The etched samples were studied under optical microscopy (OM) and scanning electron microscopy (SEM) equipped with energy dispersive spectroscopy (EDS).

### 2.2 Microhardness Testing

The microhardness tests were carried out on the polished samples. The microhardness tests were carried out using Zwick/Roell ZHV $\mu$  microhardness tester (Vickers hardness) based on ASTM 384 [24]. The microhardness test was carried out with a load of 200gf, at dwelling time of 10 seconds and space between indentation of 120  $\mu$ m. Three sets of indentation patterns were produced each from the top to the base of the clad region. Indentation patterns were made because of the clad width which is as a result of the multiple-track deposition so as to establish a more accurate hardness value per sample. Figure 2 shows a typical microhardness pattern produced on a sample of deposited 17-4 PH stainless steel.

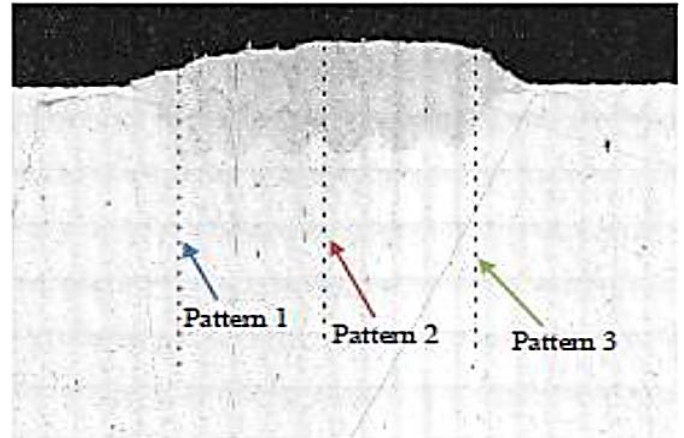


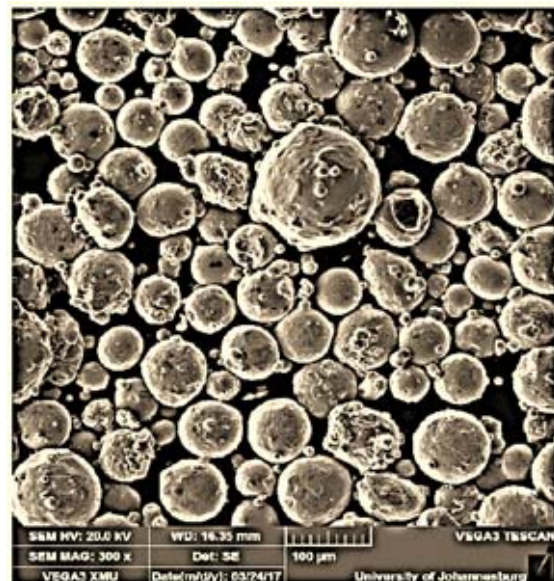
Fig. 2. A Typical Microhardness Indentation Pattern image

### 2.3 Wear Testing

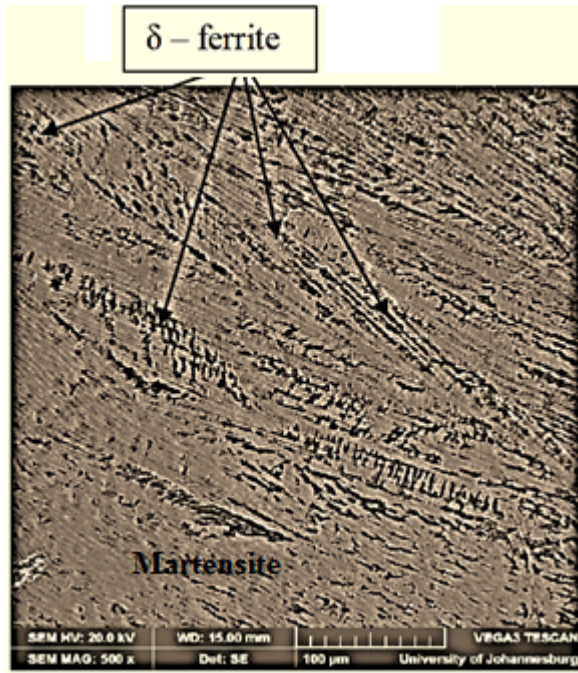
The wear resistance tests were carried out under dry condition using a ball-on-disc arrangement on ANTON PAAR-tribometer, wear tester equipment. A 6mm diameter alumina-stainless steel ball was used under the test condition of a load of 10 N, acquisition rate of 100 Hz, at a time of 16 minutes 40 seconds with a total test distance of 31.406 m under relative humidity of 50% and ambient temperature of 25°C. The wear test was carried out according to ASTM G 99-05 [25]. The analysis of the wear scars was carried out using scanning electron microscopy (SEM).

## 3. RESULTS AND DISCUSSION

The optical micrograph of the 17-4 PH stainless steel powder used in this study is shown in Figure 3 (a). The optical micrograph of a deposited sample at laser power of 1000 W is shown in Figure 3 (b). The microstructure of the 17-4 PH SS consists of delta ( $\delta$ ) ferrite formed in matrix of martensite.



(a)



(b)

**Fig. 3.** Optical Micrograph of (a) 17-4 PH SS metallic powder and (b) 17-4 PH SS Microstructure

### 3.1. Microhardness Characterization

Microhardness tests results showed in Figure 4. The average hardness value was found to initially decreased, then increased and again decreased as the laser power was further increased. The initial high hardness values experienced at lower laser power could be due to improper melting of the powder particles as well as rapid solidification of the melt pool which produced a higher microhardness value. The rapid cooling is associated with the use of low energy density in LMD process [26]. At lower energy density, which is the case at lower laser power in this study results in the formation of small volume of melt pool that solidified very quickly. As the laser power was increased, there is better melting of the powder particle that caused the microhardness value to be reduced. As the laser power was further increased, the micro hardness was also increase. This was due to proper melting of the powder particle and the higher hardness observed may be indicative of the actual microhardness value. The precipitates of delta ( $\delta$ ) ferrite and copper precipitates were seen in the microstructure of all the samples. The delta ferrite seen at lower laser power of 1800 W is finer than those seen at higher laser powers of 2200 W and 2600 W. This could be due to much rapid solidification of fully melted powder particles and smaller volume of melt pool thereby resulting in a higher microhardness value at that laser power. As the laser power was further increased, the microhardness value began to reduce again. The reason for this may be due to coarser delta ferrite seen in the microstructure that was produced due to much slower solidification rate of larger melt pool produced at larger laser power.

This caused the microhardness values to be decreased as the laser power was further increased [27].

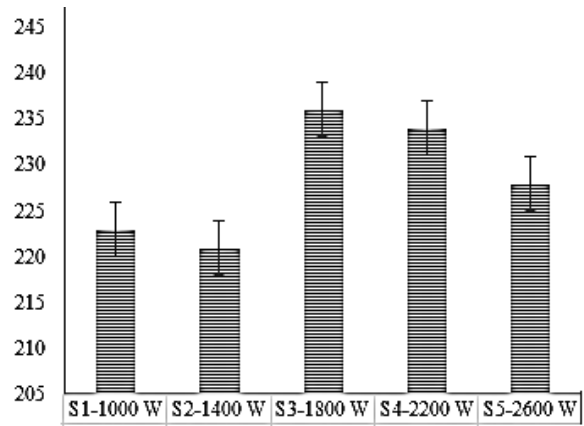


**Fig. 4.** Bar chat of the average hardness values of all samples at different laser power

### 3.2 Wear Characterization

Dry sliding wear test was carried out on all deposited samples. The worn surfaces (wear track) of the samples were examined and analysed using scanning electron microscopy (SEM). The wear of the samples was characterized by particle spallation and plastic flow. The wear volume and wear rate of deposited samples were determined in all the samples using the equations 1. and 2. as contained in the equipment manual of the Anton Paar-tribometer wear test equipment used [28].

$$v = 2\pi R \left[ r^2 \sin^{-1} \left( \frac{d}{2r} \right) - \frac{d}{4} (4r^2 - d^2)^{\frac{1}{2}} \right] \quad (1)$$

$$Wr = \frac{v}{Fa} \quad (2)$$

Where,  $v$  = wear volume ( $m^3$ ),  $R$  = wear track radius (mm),  $r$  = radius of the ball (mm),  $d$  = wear track width (mm),  $Fa$  = applied load (N),  $Wr$  = wear rate ( $m^2/N$ ), and  $l$  = total test distance (m).

The schematic diagram of the wear test process is shown in Figure 5. The results of the wear tests are presented in Table 2. The bar chart of the wear volume and wear rate is shown in Figure 6. The wear volume and wear rate were found to decrease with increase in laser power as shown in Figure 6. This may be as a result of decreasing hardness behaviour that was observed as the laser power was increased that may have improved the wear resistance behaviour. The sample deposited at the highest laser power of 2600 W was observed to have experienced the lowest wear volume and wear rate were recorded to be  $1.046 \times 10^{-6} m^3$  and  $3.3306 \times 10^{-9} m^2/N$  respectively. The highest wear rate and wear volume were experienced in sample deposited at a lower laser power of 1400 W with wear

volume of  $1.1566 \times 10^{-6} \text{ m}^3$  and wear rate of  $3.6828 \times 10^{-9} \text{ m}^2/\text{N}$ .

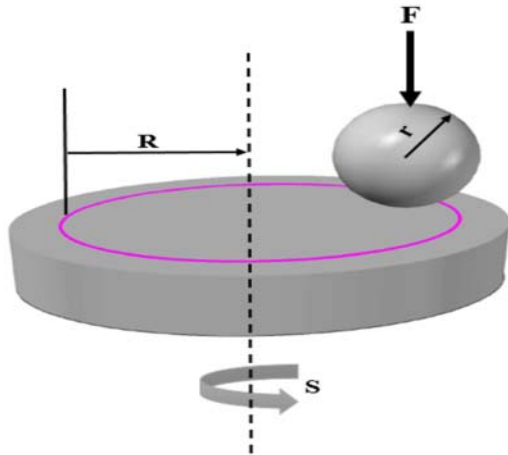


Fig. 5. Typical ball-on-disc setup indicating the normal force applied on the ball.

Table 2. Wear Track Analysis and Evaluation

Samples (laser power)	Wear track radius, R (mm)	Wear Volume, V( $\times 10^{-6} \text{ m}^3$ )	Total test distance, l, (m)	Wear Rate, ( $\times 10^{-9} \text{ m}^2/\text{N}$ )
S2 (1400 W)	2	1.1566	31.406	3.6828
S3 (1800 W)	2	1.1460	31.406	3.6491
S5 (2600 W)	2	1.0460	31.406	3.3306

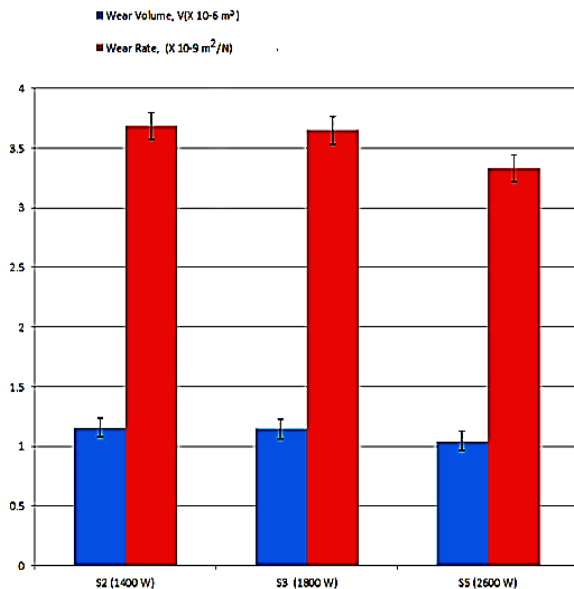


Fig. 6. Bar Chart showing the relationship between the laser powers, the wear volume and the wear rate of deposited samples

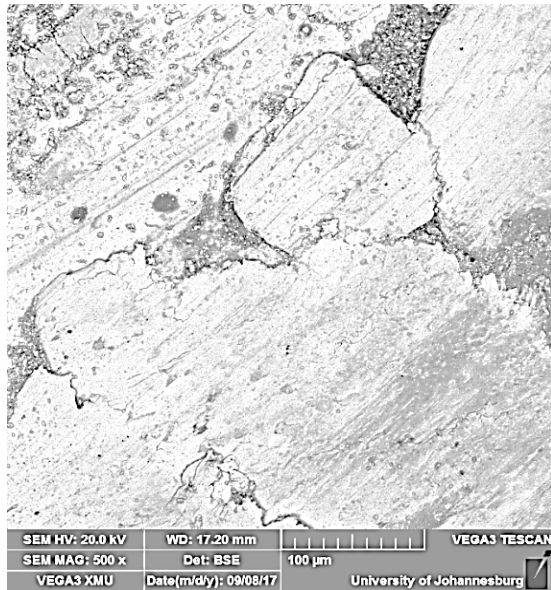
The sample deposited at a laser power of 1800 W was observed to exhibit wear volume of  $1.146 \times 10^{-6} \text{ m}^3$  and wear rate of  $3.6491 \times 10^{-9} \text{ m}^2/\text{N}$ . It can be observed

from the wear result analysis that wear rate is inversely proportional to the laser power. The reason for better wear resistance behaviour that was observed in the sample at higher laser power can be linked to not too high microhardness value that was recorded for the samples. High hardness results in brittleness of the samples at lower laser power of 1400 W that promotes spallation and breakage in the deposit during sliding wear process that promoted an increase in material removal through more scratching produced by the chipped material that changed the wear action from two body to three body wear process [29]. The relatively high microhardness seen at higher laser power may have promoted the improved wear resistance due to high quantity of martensitic microstructure with the formation of coarser delta ( $\delta$ ) ferrite and copper precipitates. The SEM micrographs of the worn track at different laser power are shown in figure 7 (a), 7 (b) and 7 (c). The wear track of the sample at a laser power of 2600 W (Figure 7a) showed a better worn surface when compared to the wear track at 1800 W (Figure 7b) and 1400 W (Figure 7c). The powdery surface in Figure 7a showed that the deposited material is not too hard and during the sliding wear operation, smaller particles of the deposit are chipped off and ground in to fine powder that further prevented the wear action as the wear action progressed. The ground powder served as a powder lubricant that inhibited the further wear action similar to what was observed in the literature [29]. The wear track at lower laser power of 1400 W was characterized with higher hardness and more brittle grain structure as shown in Figure 7b, which resulted in chipping of larger grain particles. The higher hardness of this sample at lower laser power cause the breakage of larger grain particle which aggravated the wear process thereby causing more damage to the worn track during the wear process. The wear resistance of the sample produced at a laser power of 1400 W was seen to be the highest even though the microhardness was the lowest. The reason for this behaviour may be due to the presence of unmelted powder particles in the deposit which was easily chipped off during the sliding wear process and also aggravating the wear process.

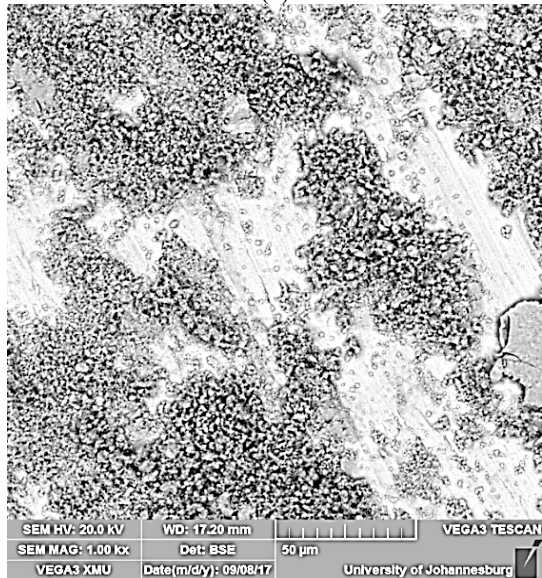
#### 4. CONCLUSION

The microhardness and the wear resistance properties of laser metal deposited 17-4 PH stainless steel were investigated in this study. The following conclusions are drawn from this study:

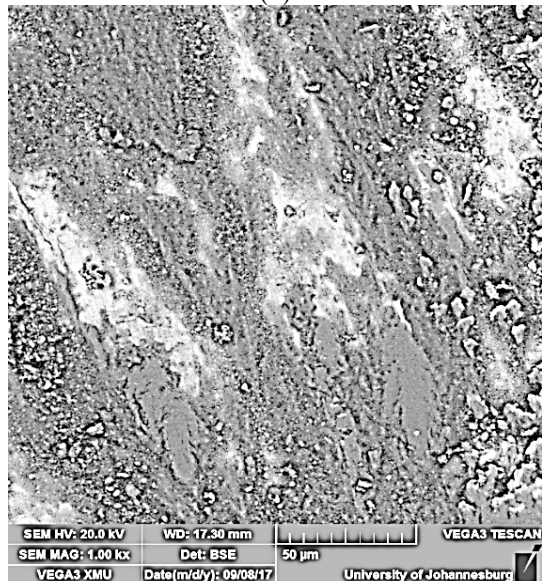
1. The microstructure consists of delta ( $\delta$ ) ferrite precipitates in the matrix of martensite that change from fine to coarse grains of delta ferrite as the laser power was increased.



(a)



(b)



(c)

**Fig. 7.** SEM Images of worn track of deposited 17-4 PH SS at laser power of (a) 2600 W (b) 1800 W and (c) 1400 W.

2. The microhardness was found to initially decrease, increase and then decrease when the laser power was increased. This initial fluctuation of the microhardness was attributed to improper melting of the powder at lower laser power, causing the erratic microhardness behaviour at lower laser powers.
3. The wear resistance behaviour was seen to improve as the laser power was increased. This showed that the optimum processing parameter for improved wear resistance behaviour is at a laser power of 2600 W based on the processing parameters considered in this study.

## ACKNOWLEDGEMENTS

The author acknowledges financial support of the Global Excellent and Stature (GES), University of Johannesburg and The National Laser Centre Council for Scientific and Industrial Research (NLC-CSIR) in Pretoria, South Africa for the rental pool grant

## NOMENCLATURE

LMD - Laser Metal Deposited  
 PH – Precipitation Hardened  
 SS – Stainless Steel  
 SEM – Scanning Electron Microscopy  
 EDS – Energy Dispersive Spectroscopy  
 $\delta$ - delta ferrite

## REFERENCES

- [1] **Yoo W-D., Lee J-H., Youn K-T., Rhyimd Y-M.,** *Study on the Microstructure and Mechanical Properties of 17-4 PH Stainless Steel depending on Heat Treatment and Aging Time*, Solid State Phenomena., 118, 2006 pp. 15-20.
- [2] **Smith, W.F.,** *Structure and Properties of Engineering Alloys*, 2nd ed., McGraw-Hill, Inc. New York, USA, 1993, pp. 328-335.
- [3] **Mahamood R. M., Akinlabi E. T.,** *Advanced Noncontact Cutting and Joining Technologies: Micro- and Nano-manufacturing*, Springer Science Publisher, Switzerland, 2018.
- [4] **Mahamood R.M., Akinlabi E.T, Shukla M. and Pityana S.,** *Revolutionary additive manufacturing: an overview*, Lasers in Engineering, 27, 2014, pp. 161-178.
- [5] **Stern A., Rosentha Y., Berger A., Ashkenazi D.,** *Additive Manufacturing - From Fundamentals To Applications*, Annals Of “Dunarea De Jos” University,

- Fascicle Xii Welding Equipment and Technology, 28, 2017 pp. 51-58.
- [6] **Rosenthal A., Tiferet E., Ganor M., Stern A.,** *post-Processing Of AM-SLM AlSi10Mg Specimens: Mechanical Properties And Fracture Behaviour*, Annals Of “Dunarea De Jos” University, Fascicle Xii Welding Equipment and Technology, 26, 2015 pp. 33-38.
- [7] **Rosenthal I., Tiferet E., Ganor M., Stern A.,** *Selective Laser Melting Additive Manufacturing: AlSi10Mg Powder Characterization*, Annals Of “Dunarea De Jos” University, Fascicle Xii Welding Equipment and Technology, 25, 2014, pp. 35-40
- [8] **Rosenthal I., Sharon R., Shwartzman Z., Stern A.,** *Hatching Strategy: 3D Visualization Model For Powder Bed Based Additive Manufacturing With Focused Beams*, Annals Of “Dunarea De Jos” University, Fascicle Xii Welding Equipment and Technology, 25, 2014, pp. 13-18.
- [9] **Berger A., Sharon Y., Ashkenazi D., Stern A.,** *Test Artefact For Additive Manufacturing Technology: FDM and SLM Preliminary Results*, Annals Of “Dunarea De Jos” University, Fascicle Xii Welding Equipment and Technology, 27, 2016, pp. 29-37.
- [10] **Mahamood R. M., Akinlabi E. T.,** *Effect of Processing Parameters on Wear Resistance Property of Laser Material Deposited Titanium -Alloy Composite*, Journal of Optoelectronics and Advanced Materials (JOAM), 17(9-10), 2015, pp. 1348 - 1360.
- [11] **S. Pityana, R. M. Mahamood, E. T. Akinlabi, and M. Shukla,** (2013). Effect of gas Flow Rate and powder flow rate on Properties of Laser Metal Deposited Ti6Al4V. 2013 International Multi-conference of Engineering and Computer Science (IMECS 2013), March 2013. 848-851.
- [12] **M. Shukla, R. M. Mahamood, E. T. Akinlabi and S. Pityana,** (2012). Effect of Laser Power and Powder Flow Rate on Properties of Laser Metal Deposited Ti6Al4V. World Academy of Science and Technology, vol.6, 44-48.
- [13] **Mahamood R.M., Akinlabi E.T., Owolabi M.G.** *Laser Metal Deposition Process for Product Remanufacturing*. In: Gupta K. editor. Advanced Manufacturing Technologies. Springer, Switzerland 2017, pp. 267-291.
- [14] **Mahamood R.M.,** *Laser Metal Deposition Process of Metals, Alloys, and Composite Materials*, Springer, Switzerland, 2018.
- [15] **Mahamood R.M., Akinlabi E. T.,** *Functionally Graded Materials*, Springer Science Publisher, Switzerland, 2017.
- [16] **Mahamood, R. M., Akinlabi, E. T.,** *Laser Additive Manufacturing*. In *Advanced Manufacturing Techniques Using Laser Material Processing*, IGI Global 2016, pp. 1-23.
- [17] **Yu, J., Rombouts, M., Maes, G.,** *Cracking behaviour and mechanical properties of austenitic stainless steel parts produced by laser metal deposition*. Materials & Design, 45, 2013, pp. 228-235.
- [18] **Zhang K, Wang S, Liu W, Shang X.,** *Characterization of stainless steel parts by Laser Metal Deposition Shaping*. Materials and Design, 55, 2014, pp. 104 – 119.
- [19] **Yadollahi A, Shamsaei N, Thompson S.M, Seely D.W.,** *Effects of process time interval and heat treatment on the mechanical and microstructural properties of direct laser deposited 316L stainless steel*. Journal of Materials Science and Engineering. A644. 2015, pp. 171 – 183.
- [20] **Guo P, Zou B, Huang C, Gao H.,** *Study on microstructure, mechanical properties and machinability of efficiently additive manufactured AISI 316L Stainless steel by high-power direct laser deposition*. Journal of Material Processing Technology. 240, 2016, pp. 12 -22.
- [21] **Wang Z, Palmer T.A, Beese A.M.,** *Effect of processing parameters on microstructure and tensile properties of austenitic stainless steel 304L made by directed energy deposition additive manufacturing*. Acta Materialia, 110, 2016, pp. 226 – 235.
- [22] **Bayode A., Akinlabi E.T., Pityana S.,** *Characterization of laser metal deposited 316L stainless steel*, Lecture notes in engineering and computer science, 1, 2015, 925-928.
- [23] **Bayode A., Akinlabi E.T., Pityana S.,** *Microstructure and microhardness of 17-4 PH stainless steel made by laser metal deposition*. Lecture notes in engineering and computer science, 1 2016, 812-814.
- [24] ASTM E384-11e1, *Standard test method for Knoop and Vickers Hardness of materials*, ASTM international book of standards 03(01) 2011.
- [25] ASTM Standard G99-05, *Standard Test Method for Ball-on-disc Sliding Wear*, Annual Book of ASTM Standard 2007.
- [26] **Mahamood R. M., Akinlabi E. T., Shukla M. Pityana S.,** *Characterizing the Effect of Laser Power Density on Microstructure, Microhardness and Surface Finish of Laser Deposited Titanium Alloy*. Journal of Manufacturing Science and Engineering, 135(6), 2013, 064502-064502-4. doi:10.1115/1.4025737.
- [27] **Adeyemi, A. A., Akinlabi, E. T., Mahamood, R. M., Sanusi, K. O., Pityana, S., Tlotleng, M.,** *Influence of laser power on microstructure of laser metal deposited 17-4 PH stainless steel*. In IOP Conference Series: Materials Science and Engineering, 225(1) 2017, pp. 012028).
- [28] Pin –on – disk ANTON PAAR Tribometer (GmbH) Manual, Strasse 208054, Austria.
- [29] **Mahamood R.M., Akinlabi E.T, Shukla M. and Pityana S.,** *Scanning Velocity Influence on Microstructure, Microhardness and Wear Resistance Performance on Laser Deposited Ti6Al4V/TiC Composite*, Materials and Design, 50, 2013, pp. 656-666.